A. Säynätjoki, K. Vynck, M. Mulot, D. Cassagne, J. Ahopelto, and H. Lipsanen. 2008. Efficient light coupling into a photonic crystal waveguide with flatband slow mode. Photonics and Nanostructures – Fundamentals and Applications, in press, doi:10.1016/j.photonics.2008.03.001.

© 2008 Elsevier Science

Preprinted with permission from Elsevier.

Available online at www.sciencedirect.com
ScienceDirect
ELSEVIER
PHOTONICS AND NANOSTRUCTURES
Fundamentals and Applications
www.elsevier.com/locate/photonics

Efficient light coupling into a photonic crystal waveguide with flatband slow mode

A. Säynätjoki [a,*], K. Vynck [b], M. Mulot [a,c], D. Cassagne [b], J. Ahopelto [c], H. Lipsanen [a]

[a] *Helsinki University of Technology (TKK), Department of Micro and Nanosciences, Micronova, Tietotie 3, FIN-02015 Espoo, Finland*
[b] *Groupe d'Etude des Semiconducteurs, UMR 5650 CNRS - Université Montpellier II, CC074 Place Eugne Bataillon, 34095 Montpellier Cedex 05, France*
[c] *VTT Information Technology, Micronova, P.O. Box 1208, FIN-02044 VTT, Finland*

Received 21 January 2008; received in revised form 13 March 2008; accepted 21 March 2008

Abstract

We design an efficient coupler to transmit light from a strip waveguide into the flatband slow mode of a photonic crystal waveguide with ring-shaped holes. The coupler is a section of a photonic crystal waveguide with a higher group velocity, obtained by different ring dimensions. We demonstrate coupling efficiency in excess of 95% over the 8 nm wavelength range where the photonic crystal waveguide exhibits a quasi-constant group velocity $v_g \approx c/37$ and observe a more than 12-fold intensity enhancement in the slow-light waveguide. An analysis based on the small Fabry–Pérot resonances in the simulated transmission spectra is used for studying the effect of the coupler length and for evaluating the coupling efficiency in different parts of the coupler. The mode conversion efficiency within the coupler is more than 99.7% over the wavelength range of interest. The parasitic reflectance in the coupler, which depends on the propagation constant mismatch between the slow mode and the coupler mode, is lower than 0.6%.
© 2008 Elsevier B.V. All rights reserved.

PACS : 42.15.Eq; 42.70.Qs; 42.82. −m; 42.82.Cr; 42.82.Et; 42.82.Gw

Keywords: Guided waves; Integrated optics materials; Optical systems design; Waveguides; Photonic integrated circuits; Dispersion; Photonic crystals

1. Introduction

Photonic crystal waveguides (PhCWs) exhibit slow optical modes with group velocities at least one order of magnitude smaller than in conventional waveguides [1–5]. Enhanced nonlinearity effects have been demonstrated for slow modes, which may allow scaling down the size of active integrated optics devices [6,7]. Slow modes can be used in telecommunication systems provided that they have sufficiently low group velocity dispersion (GVD), and PhCWs with such flatband slow modes have recently been designed [8–10]. We have designed a waveguide based on a photonic crystal with ring-shaped holes (RPhCW) with low GVD and group velocity $v_g \approx c/37$ over a wavelength range of several nanometers [11]. The feasibility of the RPhCW was shown in [12], where we observed slow-light propagation in an RPhCW fabricated on a silicon-on-insulator substrate.

Efficient coupling between waveguides with different group velocities is not trivial [13–16]. Transmission from strip waveguides (SWs) to slow modes in PhCWs

* Corresponding author.
E-mail address: antti.saynatjoki@tkk.fi (A. Säynätjoki).

1569-4410/$ – see front matter © 2008 Elsevier B.V. All rights reserved.
doi:10.1016/j.photonics.2008.03.001

Please cite this article in press as: A. Säynätjoki, et al., Efficient light coupling into a photonic crystal waveguide with flatband slow mode, Photon Nanostruct: Fundam Appl (2008), doi:10.1016/j.photonics.2008.03.001

can be improved by optimizing the termination of the PhCW [13], tapering the PhCW [15] and by using high group velocity PhCWs at both ends of the slow-light PhCW [16]. In these examples, efficient coupling into slow modes in PhCWs was achieved with couplers significantly shorter than required for adiabatic mode conversion. De Sterke et al. [17] and Velha et al. [18] showed that perfect coupling could be achieved by utilizing the interference between the forward and backward propagating modes in the coupler. Hugonin et al. [19] noticed the appearance of a transient zone a few lattice periods long at the interface between PhCW sections of different group velocities, where light is smoothly slowed down as it penetrates the slow-light waveguide, and they demonstrated efficient mode conversion in such a structure. This approach makes it possible to optimize the different interfaces of the slow-light device independently.

In this paper we design an efficient coupler into the slow, dispersion engineered mode with a nearly constant v_g in the RPhCW presented in [11]. We present a simple way of studying coupling efficiencies in different parts of the coupler, based on the small F–P resonances in the transmission spectrum.

2. Coupler design

2.1. Group velocity in RPhC waveguides

Fig. 1 shows a schematic of an RPhCW defined by one missing row of holes in an otherwise perfect RPhC. The RPhC is a triangular lattice of rings with a lattice constant a. The ring is defined by two parameters, ring outer and inner radii R_{out} and R_{in}, respectively. The RPhCW is coupled to SWs with width w at the interface. The parameter d defines the position at which the RPhCW is terminated.

Band structures of the RPhCWs are calculated using the plane wave expansion (PWE) method described in [20]. The PWE simulations yield dispersion relations $u(\beta)$, where u is the normalized frequency $u = a/\lambda$ and β is the propagation constant. The group velocity v_g is

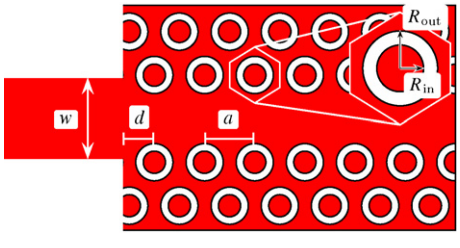

Fig. 1. Schematic of a W1 RPhC with an input strip waveguide.

defined as

$$v_g = \frac{d\omega}{d\beta} = \frac{2\pi c}{a}\frac{du}{d\beta}. \quad (1)$$

Therefore, v_g is directly proportional to the slope of the dispersion curve in Fig. 2, where we plot the dispersion relation of the even TE polarized mode (electric field in the propagation plane) in RPhCWs with different values of R_{out}. The ring width is kept constant at $R_{out} - R_{in} = 0.15a$. The simulations were carried out in 2D for the TE polarization. An effective index of the dielectric material equal to $n_{eff} = 3.178$ was used, corresponding to the effective refractive index of a 400 nm thick silicon ($n_{Si} = 3.48$) slab on silica ($n_{SiO_2} = 1.46$) at the wavelength of 1550 nm.

We have demonstrated in our previous work that an RPhCW with $R_{out} = 0.385a$ and $R_{in} = 0.235a$ exhibits a flatband mode with a quasi-constant and relatively low group velocity $v_g \approx c/37$ over a wavelength range of 8 nm [11]. The frequency range corresponding to the nearly constant v_g is between the normalized frequencies $u = 0.250$ and 0.2512 and it is highlighted in Fig. 2. The v_g values in this paper are given for this frequency range, unless the frequency or propagation constant range is explicitly specified. With a lattice constant $a = 392$ nm, which we will use later in this paper, the range of nearly constant v_g lies between wavelengths 1560 and 1568 nm.

For all waveguides in Fig. 2, the even mode is in the index-guided regime with $v_g \approx c/3.8$ when $\beta < 0.32(2\pi/a)$. When approaching the Brillouin zone edge at $\beta = 0.5(2\pi/a)$, the mode becomes diffraction-guided: v_g decreases and eventually vanishes when $\beta = 0.5(2\pi/a)$. If R_{out} is decreased, the air-fill factor of

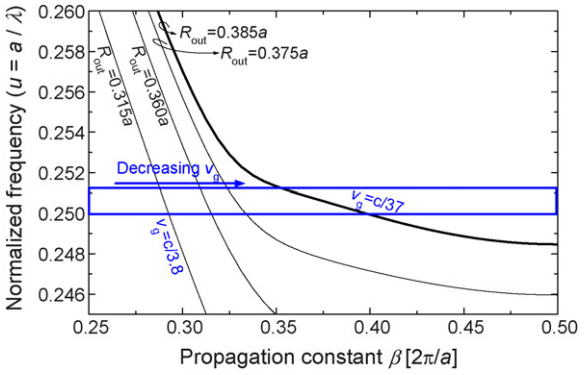

Fig. 2. Dispersion relation of the even mode in RPhCWs with different outer radius R_{out}. The ring width $R_{out} - R_{in} = 0.15a$ for all waveguides. In the normalized frequency range within the frame, the average group velocity decreases from $v_g = c/3.8$ when $R_{out} = 0.315a$ to $v_g = c/37$ when $R_{out} = 0.385a$.

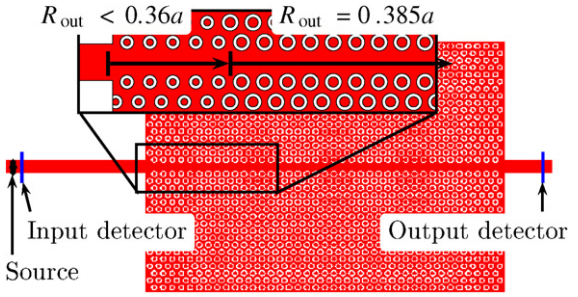

Fig. 3. Schematic image of the coupler design. A slow-light RPhCW is coupled to SWs through RPhCWs with smaller R_{out}, i.e., with higher v_g. The inset shows the beginning of the RPhCW. The source and detector configuration in FDTD simulations is also shown in the schematic.

the RPhCW decreases, therefore, the dispersion curve of the guided mode is shifted to smaller frequencies. Consequently, the average group velocity within the frequency range of interest can be changed from $v_g = c/3.8$ with $R_{out} = 0.315a$ to $v_g = c/37$ with $R_{out} = 0.385a$.

2.2. Optimization of the coupler

The structure we consider is shown schematically in Fig. 3. The slow-light waveguide is sandwiched between two couplers, which consist of RPhCWs with $R_{out} < 0.36a$ and are coupled with strip waveguides. We start the coupler design by optimizing the coupling of light from the SWs to the coupler.

The transmission T of the couplers is obtained using the finite-difference time-domain (FDTD) method [21] by calculating the power flux ratio through two line detectors placed on the input and output SWs. The positions of the source (fundamental mode of the SW) and detectors are shown in Fig. 3. The 2D FDTD simulations were carried out for the TE polarization using an effective refractive index $n_{eff} = 3.178$, as in the case of the PWE simulations.

First, we optimize the SW width and the termination parameter d with a series of FDTD calculations on the transmission T through a $10a$ long RPhCW sandwiched between two SWs. We find that a SW width $w = 1.6a$ and termination parameter $d = 0.625a$ yield $T > 90\%$ over the frequency range of interest when $R_{out} \leq 0.355a$. In the rest of the paper, the SW-coupler interface will be defined by these parameters.

In Fig. 4, group velocity at $u = 0.250$ is plotted as a function of R_{out}, together with the transmission through a $10a$ long RPhCW sandwiched between two SWs. For the RPhCW with $R_{out} = 0.385a$, transmission is only 52% at $u = 0.250$. T increases with increasing group

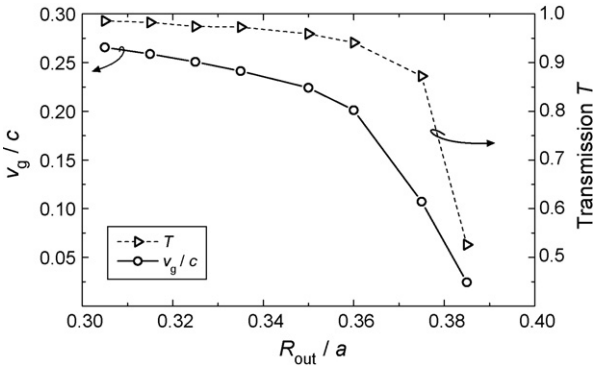

Fig. 4. Group velocity in the RPhCW (solid line) and the transmission of a $10a$ long RPhCW sandwiched between two strip waveguides (dashed line) as a function of R_{out} at the normalized frequency $u = 0.250$.

velocity, being more than 98% when $R_{out} \leq 0.315a$ and $v_g > c/4$. Therefore, we choose $R_{out} = 0.315a$ for the coupler.

In [19], Hugonin et al. showed efficient coupling of light between two PhCWs with large group velocity mismatch (slowdown factor of ¿20) by using a modified lattice parameter at their interface. The adaptation of the lattice parameter is necessary when the slowdown factor is large. In our case, the coupler and the RPhCW have group velocities $c/3.8$ and $c/37$, respectively, i.e., the slowdown factor is only ≈ 10, so that we expect an efficient coupling without such modification. We, therefore, consider an abrupt change of R_{out} at the interface between the coupler and the slow-light waveguide. In our initial structure, we use a coupler length of $5a$. We will discuss the effect of the length of the couplers later in this paper.

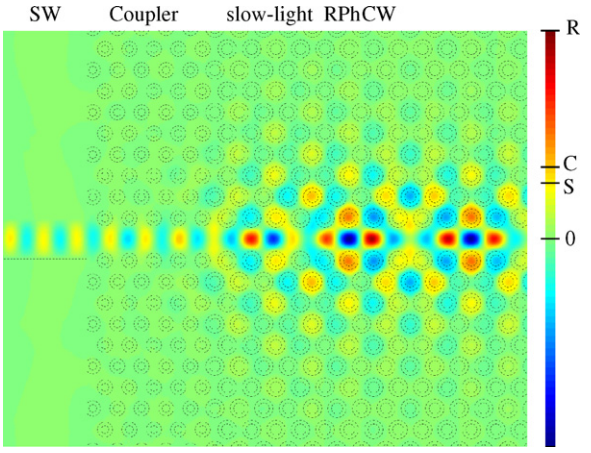

Fig. 5. The H_z field in the input coupler with a continuous wave source operating at frequency $u = 0.2506$. The zero point and maxima of H_z in the SW (S), coupler (C) and RPhCW (R) are marked onto the colorbar.

Fig. 5 shows the amplitude of the magnetic field in the coupler with a continuous wave input at a normalized frequency $u = 0.2506$. The conversion from the coupler mode into the wider slow mode takes place within a few lattice periods of the coupler-RPhCW interface, which confirms the existence of a transient zone at the interface between sections with different group velocities [19]. Fig. 5 also shows a 3.5-fold increase in the field strength (12.25(increase in intensity) between the SW and the slow-light waveguide. The spectral characteristics of the coupling will be discussed in the next section.

3. Results and discussion

3.1. Transmission properties

Fig. 6 shows the transmission spectra of a $50a$ long slow-light RPhCW with and without couplers (T_{opt} and T_{ref}, respectively). Transmission through the RPhCW with $R_{out} = 0.315a$ sandwiched between SWs (T_{cpl}) is also plotted into Fig. 6 in order to show the transmission between the SWs and the couplers. The PWE calculated group index $n_g = c/v_g$ in the RPhCW with $R_{out} = 0.385a$, presented in [11], is plotted into the same graph. All the curves are plotted as a function of wavelength λ with a lattice constant $a = 392$ nm, which yields a cut-off wavelength of 1575 nm.

T_{opt} is higher than 95% over the wavelength range of nearly constant v_g between 1560 and 1568 nm. The device thus provides both high transmission efficiency and low group velocity dispersion for a broadband optical signal, which is important if slow-light waveguides are considered to be used in data transmission systems.

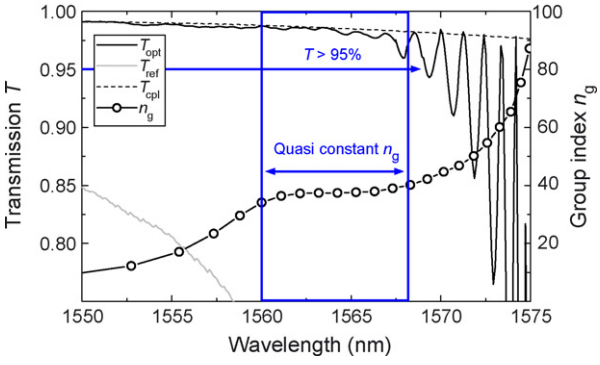

Fig. 6. FDTD simulated transmission spectra through a $50a$ long RPhC waveguide with $R_{out} = 0.385a$ and $a = 392$ nm, with and without couplers at both ends (T_{opt} and T_{ref}, respectively). T_{cpl} is the transmission spectrum of a $10a$ long RPhCW with $R_{out} = 0.315a$ (i.e., a waveguide similar to the couplers) sandwiched between SWs. Group index $n_g = c/v_g$ is deduced from the PWE simulations [11].

Up to the wavelength 1567 nm, T_{opt} is very close to T_{cpl}. Only small oscillations are seen in the spectrum, with their period varying as a function of the group index of the RPhCW. These oscillations are F–P resonances due to reflections between the two coupler-RPhCW interfaces. In the next section we will show that these F–P oscillations are a sensitive indicator of mode conversion efficiency and reflections in the coupler, and therefore, constitute an efficient way of studying the various coupling mechanisms in such structures.

3.2. Fabry–Pérot analysis

PhCW modes within the photonic band gap are necessarily lossless in 2D simulations, as out-of-plane losses do not exist and in-plane losses are prohibited by the PhC. Therefore, non-ideal transmission in our simulation is induced by in-plane scattering and/or by parasitic back reflection at each waveguide interface.

3.2.1. Mode conversion efficiency

The transmission of a lossless F–P cavity is equal to unity at resonance [23]. T_{opt} should, therefore, be equal to T_{cpl} at each resonance, provided that the coupler converts the slow mode properly into the coupler mode; this is the case in the transmission spectrum shown in Fig. 6 for wavelengths up to 1572 nm. For resonances at longer wavelengths, $T_{opt} < T_{cpl}$, suggesting that mode conversion is not perfect.

The efficient mode conversion experienced between PhCW sections of significantly different group velocities has been explained by the creation of a transient zone within a few lattice periods of the slow-light waveguide resulting from interferences between propagating and evanescent Bloch modes. Such transient zone is observed in Fig. 5. To get more insight on the mode conversion along the coupler, we repeat the FDTD simulation of T_{opt} with different coupler lengths m, where m is the coupler length in lattice periods a. The results are shown in Fig. 7, where we plot $T_{opt,R}/T_{cpl}$, where $T_{opt,R}$ is the linear interpolation between the points corresponding to F–P resonances in T_{opt}. Perfect mode conversion should yield $T_{opt,R}/T_{cpl} = 1$.

The coupler with a length of just $2a$ is enough to improve transmission compared to the waveguide with no couplers (compare to T_{ref} in Fig. 6). A coupler with $m = 3$ provides nearly perfect coupling in the quasi-constant group index range. With $m = 5$, transmission is enhanced between $\lambda = 1566$ and 1574 nm.

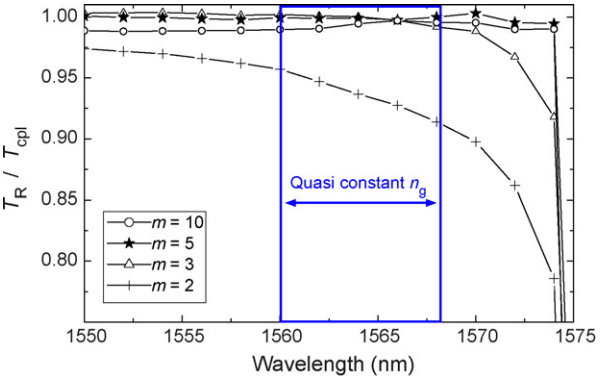

Fig. 7. A measure for mode conversion efficiency, $T_{opt,R}/T_{cpl}$, with different coupler lengths. $T_{opt,R}$ is the linear interpolation between the points corresponding to F–P resonances in the transmission spectra with a coupler with a length of m lattice periods, and T_{cpl} is the transmission spectra of the coupler sandwiched between strip waveguides.

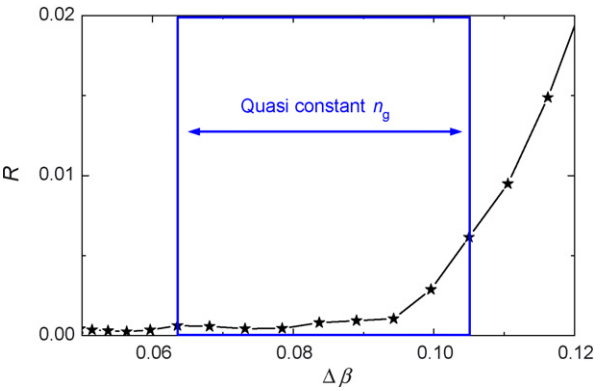

Fig. 8. Parasitic back-reflectance R as a function of propagation constant mismatch $\Delta\beta$ with a $5a$ long coupler. The wavelength range of the figure is from about 1555 to about 1570 nm, the quasi-constant n_g region is drawn between 1560 and 1568 nm and the scatter symbols have an interval of 1 nm.

Further increase in the coupler length maintains the excellent transmission, which shows that efficient coupling occurs when the evanescent modes excited at each end of the coupler do not overlap and interfere destructively [19]. The coupler length needed for this is $5a$. The weak transmission variations that are observed for longer couplers correspond to F–P oscillations in the coupler [17]. However, these oscillations are not dominant in our case. For a coupler length of $5a$, we see that the mode conversion losses are lower than 0.3% in the wavelength range of quasi-constant n_g. $T_{opt,R}$ drops near cut-off for all coupler lengths, indicating that a more complicated coupler might be needed for higher n_g [15,19].

3.2.2. Back-reflectance

The signature of the back reflections are the F–P oscillations in the transmission spectrum, which can be seen in T_{opt}. In this case, the RPhCW can be regarded as a symmetric, lossless F–P cavity. The reflectance R at the ends of such a cavity can be deduced from the F–P oscillations in the transmission spectrum as [22]

$$R = \frac{\sqrt{T_R/T_A} - 1}{\sqrt{T_R/T_A} + 1}, \tag{2}$$

where T_R and T_A are the transmission at resonance and antiresonance, respectively.

The amplitude of the F–P oscillations in Fig. 6 increases at higher wavelengths already within the nearly constant n_g regime. The oscillation amplitude is indeed a function of the propagation constant mismatch between the slow mode and the coupler mode, $\Delta\beta$. Fig. 8 shows the back-reflectance as a function of $\Delta\beta$. In the wavelength range with constant n_g, R is lower than 0.6%. It is worth noting that the F–P resonances make it extremely important to minimize the back-reflectance at the interfaces of different RPhCW sections. At antiresonance, the transmission may be strongly decreased. The back-reflectance peaks, which co-exist with each transmission dip, might be harmful in an integrated optical circuit. Transmission of light after multiple reflections at the ends of a long slow-light waveguide should also be avoided due to the large group delay. The low back-reflectance that our coupler exhibits is, therefore, essential when designing slow-light devices for photonic integrated circuits.

3.3. Discussion

The simulations in this work have been carried out in 2D to provide reliable guidelines for the design of efficient slow-light devices based on RPhCs and to study the physical phenomena involved in the coupling processes. However, it is important to discuss some of the issues that may appear in 3D space. Planar structures in 3D exhibit out-of-plane scattering and mode mixing, which may thereby be responsible for non-negligible losses. Various studies on RPhCs [11,24,25] have shown that such structures, with an extra design parameter R_{in}, are particularly suitable for tailoring of their dispersion properties. The RPhCs can, for example, be designed to exhibit polarization independent band gaps [25], which may be useful to inhibit mode mixing. We, therefore, believe that the results of this 2D study, together with the advantages of the RPhC in resolving possible 3D

issues, will help in realizing more efficient slow-light devices. Finally, we should note that the whole device in this work was designed using the W1 waveguide in a non-modified RPhC lattice with a constant line width used in our previous experimental studies [12,24]. This constitutes a further demonstration of the engineerability of the RPhC, and a reason to foresee experimental work on such devices in the near future.

4. Conclusion

We present a highly efficient coupler into a slow mode with low group velocity dispersion in a photonic crystal waveguide with ring-shaped holes. The coupler is a section of a waveguide with a different ring parameter and with an optimized interface with the strip waveguide. The slow mode of interest exhibits a quasi-constant group index of 37 ± 3 on a bandwidth of 8 nm at telecommunications wavelengths.

We introduce simple and efficient methods based on the study of transmission spectra to evaluate the coupling efficiencies in different parts of the coupler. The coupling efficiency at the interface between the strip waveguide and the coupler is higher than 98%. We show that the mode conversion efficiency in a $5a$ long coupler is more than 99.7% over the wavelength range of interest. The parasitic back-reflectance in the coupler, which depends on the propagation constant mismatch between the slow mode and the coupler mode, is smaller than 0.6% in the same wavelength range.

On the technological point of view, the coupler is very compact and it is manufacturable with a process described in our earlier work. The total transmission of the slow-light waveguide coupled to strip waveguides is higher than 95% over the 1 THz bandwidth of the dispersion tailored slow mode. Following the recent introduction of slow-light photonic crystal waveguides with low group velocity dispersion, this work constitutes an important step towards integrating such devices into photonic circuits.

Acknowledgments

This work was financed by the Academy of Finland under the PHC-OPTICS project, graduate school GETA and the European Union under project PHAT.

References

[1] M. Notomi, K. Yamada, A. Shinya, J. Takahashi, C. Takahashi, I. Yokohama, Extremely large group-velocity dispersion of line-defect waveguides in photonic crystal slabs, Phys. Rev. Lett. 87 (2001) 253902.
[2] X. Letartre, C. Seassal, C. Grillet, P. Rojo-Romeo, P. Viktorovitch, M. Le Vassor d'Yerville, D. Cassagne, C. Jouanin, Group velocity and propagation losses measurement in a single-line photonic-crystal waveguide on InP membranes, Appl. Phys. Lett. 79 (2001) 2312–2314.
[3] M. Notomi, A. Shinya, S. Mitsugi, E. Kuramochi, H-Y. Ryu, Waveguides, resonators and their coupled elements in photonic crystal slabs, Opt. Express 12 (2004) 1551–1561.
[4] H. Gersen, T.J. Karle, R.J.P. Engelen, W. Bogaerts, J.P. Korterik, N.F. van Hulst, T.F. Krauss, L. Kuipers, Real-space observation of ultraslow light in photonic crystal waveguides, Phys. Rev. Lett. 94 (2005) 073903.
[5] Y.A. Vlasov, M. O'Boyle, H.F. Hamann, S.J. McNab, Active control of slow light on a chip with photonic crystal waveguides, Nature 438 (2005) 65–69.
[6] M. Soljačić, J. Joannopoulos, Enhancement of nonlinear effects using photonic crystals, Nat. Mater. 3 (2004) 211–219.
[7] M. Roussey, M.-P. Bernal, N. Courjal, D. Van Labeke, F.I. Baida, R. Salut, Electro-optic effect exaltation on lithium niobate photonic crystals due to slow photons, Appl. Phys. Lett. 89 (2006) 241110.
[8] M.D. Settle, R.J.P. Engelen, M. Salib, A. Michaeli, L. Kuipers, T.F. Krauss, Flatband slow light in photonic crystals featuring spatial pulse compression and terahertz bandwidth, Opt. Express 15 (2007) 219–226.
[9] L.H. Frandsen, A.V. Lavrinenko, J. Fage-Pedersen, P.I. Borel, Photonic crystal waveguides with semi-slow light and tailored dispersion properties, Opt. Express 14 (2006) 9444–9450.
[10] A. Jafarpour, A. Adibi, Y. Xu, R.K. Lee, Mode dispersion in biperiodic photonic crystal waveguides, Phys. Rev. B 68 (2003) 233102.
[11] A. Säynätjoki, M. Mulot, J. Ahopelto, H. Lipsanen, Dispersion engineering of photonic crystal waveguides with ring-shaped holes, Opt. Express 15 (2007) 8323–8328.
[12] M. Mulot, A. Säynätjoki, S. Arpiainen, H. Lipsanen, J. Ahopelto, Slow-light propagation in photonic crystal waveguides with ring-shaped holes, J. Opt. A: Pure Appl. Opt. 9 (2007) S415–S418.
[13] Y.A. Vlasov, S.J. McNab, Coupling into the slow-light mode in slab-type photonic crystal waveguides, Opt. Lett. 31 (2006) 50–52.
[14] T.F. Krauss, Slow light in photonic crystal waveguides, J. Phys. D: Appl. Phys. 40 (2007) 2666–2670.
[15] P. Pottier, M. Gnan, R.M. De La Rue, Efficient coupling into slow-light photonic crystal channel guides using photonic crystal tapers, Opt. Express 15 (2007) 6569–6575.
[16] N. Ozaki, Y. Kitagawa, Y. Takata, N. Ikeda, Y. Watanabe, A. Mizutani, Y. Sugimoto, K. Asakawa, High transmission recovery of slow light in a photonic crystal waveguide using a hetero group velocity waveguide, Opt. Express 15 (2007) 7974–7983.
[17] C.M. de Sterke, J. Walker, K.B. Dossou, L.C. Bottene, Efficient slow-light coupling into photonic crystals, Opt. Express 15 (2007) 10984–10990.
[18] P. Velha, J.P. Hugonin, P. Lalanne, Compact and efficient injection of light into band-edge slow-modes, Opt. Express 15 (2007) 6102–6112.
[19] J.P. Hugonin, P. Lalanne, T.P. White, T.F. Krauss, Coupling into slow-mode photonic crystal waveguides, Opt. Lett. 32 (2007) 2638–2640.

[20] S. Johnson, J.D. Joannopoulos, Block-iterative frequency-domain methods for Maxwell's equations in a planewave basis, Opt. Express 8 (2001) 173–190.
[21] M. Qiu, F2P software, http://www.imit.kth.se/info/FOFU/PC/F2P/.
[22] A. Säynätjoki, M. Mulot, S. Arpiainen, J. Ahopelto, H. Lipsanen, Characterization of photonic crystal waveguides using Fabry–Pérot resonances, J. Opt. A: Pure Appl. Opt. 8 (2006) 502–S506.
[23] H. van de Stadt, J.M. Muller, Multimirror Fabry–Pérot interferometers, J. Opt. Soc. Am. A 2 (1985) 1363–1370.
[24] A. Säynätjoki, M. Mulot, K. Vynck, D. Cassagne, J. Ahopelto, H. Lipsanen, Properties, applications and fabrication of photonic crystals with ring-shaped holes in silicon-on-insulator, Photon. Nanostruct.: Fundam. Applic. (2007). doi:10.1016/j. photonics.2007.09.001.
[25] H. Kurt, D.S. Citrin, Annular photonic crystals, Opt. Express 13 (2005) 10316.